Electronic Supplementary Material (ESI) for Journal of Materials Chemistry A

Supplementary Information

Growth of ordered anodic SnO_2 nanochannel layers and their use for H_2 gas-sensing

A. Palacios-Padrós,[a,b,c] M. Altomare,[c,d] A. Tighineanu,[c] R. Kirchgeorg,[c] N.K. Shrestha,[c] I. Díez-Pérez,[a,b] F. Caballero-Briones,[e] F. Sanz[b,a,f] and P. Schmuki[c,g,*]

[a] *Department of Physical Chemistry, University of Barcelona, Martí i Franquès 1, 08028 Barcelona, Spain*

[b] *Institute for Bioengineering of Catalonia (IBEC), Ed. Hèlix, Baldiri i Reixac 15-21, 08028 Barcelona, Spain*

[c] *Department of Materials Science and Engineering, WW4-LKO, University of Erlangen-Nuremberg, Martensstrasse 7, D-91058 Erlangen, Germany*

[d] *Department of Chemistry, University of Milan, via Golgi 19, I-20133 Milano, Italy*

[e] *Instituto Politécnico Nacional, Laboratorio de Materiales Fotovoltaicos, CICATA-Altamira, Km 14.5 Carretera Tampico-Puerto Industrial Altamira, 89600 Altamira, México*

[f] *CIBER-BBN. Campus Río Ebro – Edificio I+D Bloque 5, 1ª planta, Poeta Mariano Esquillor s/n, 50018 Zaragoza, Spain*

[g] *Department of Chemistry, King Abdulaziz University, Jeddah, Saudi Arabia*

** Corresponding author: P. Schmuki. Fax: +49 9131 852 7575; Tel: +49 9131 852 7582;E-mail: schmuki@ww.uni-erlangen.de*

Figure S1

We found that the presence of Na_2S not only induces passivation of the tin metal but also provides an alkaline medium where hydroxyl ions contribute to a controlled dissolution of the formed oxide. During preliminary experiments, the concentration of both Na_2S and NH_4F were optimized to reach the proper equilibrium between passivation and dissolution rates, such equilibrium being the key factor to produce self-assembled nanostructured oxides.[1] Interestingly, also other fluoride sources or even chlorides were found to be successful for achieving self-organization and more open and defined top-morphology (see Fig. S4).

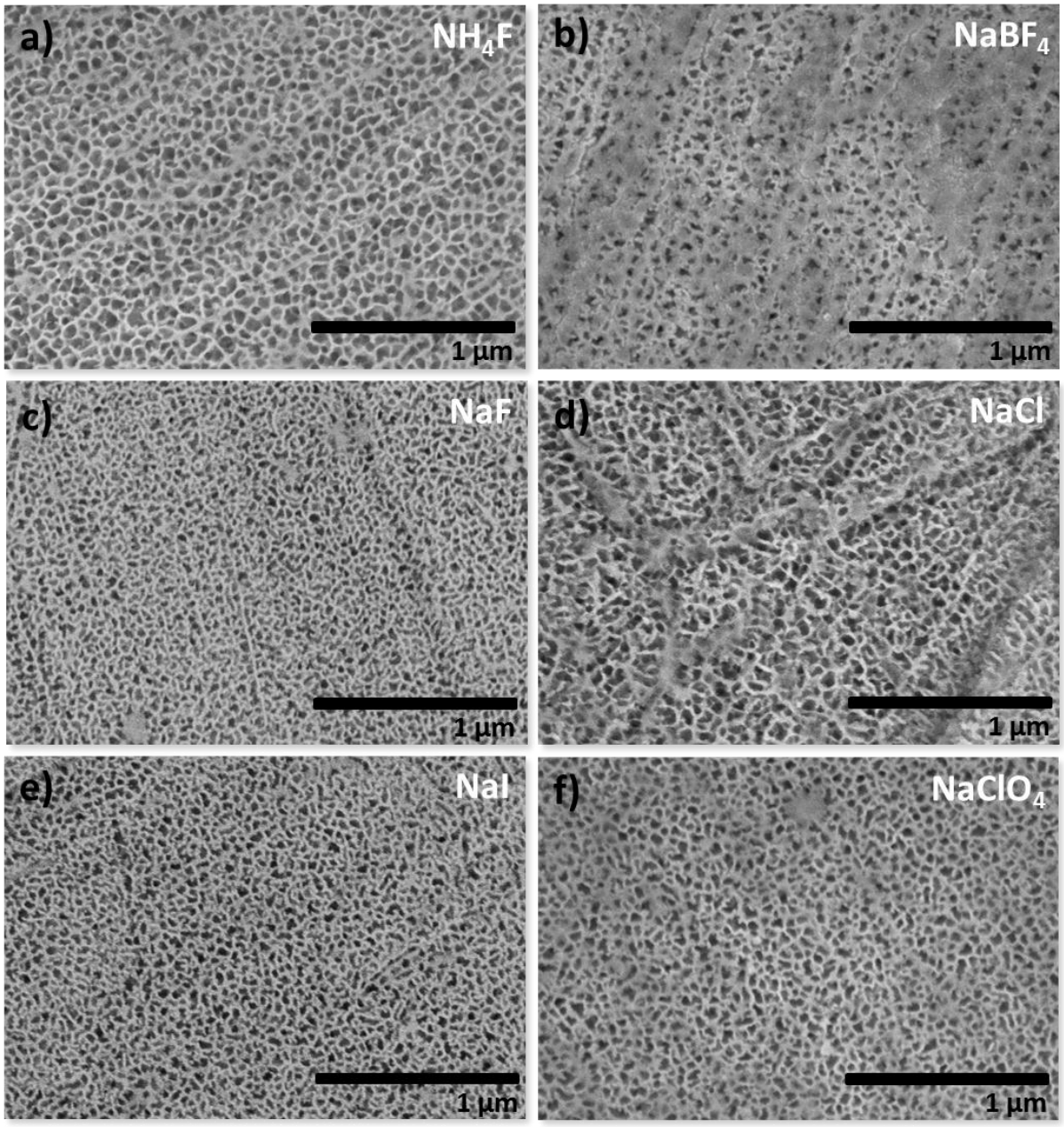

Fig. S1 Top view SEM micrograph of as-formed samples after anodization at 5 V in a 20 vol.% ethylene glycol - 80 vol.% water electrolyte containing 0.3 M Na_2S and 0.1 M a) NH_4F, b) $NaBF_4$, c) NaF, d) NaCl, e) NaI, and f) $NaClO_4$. Anodization time was 30 min.

Figure S2

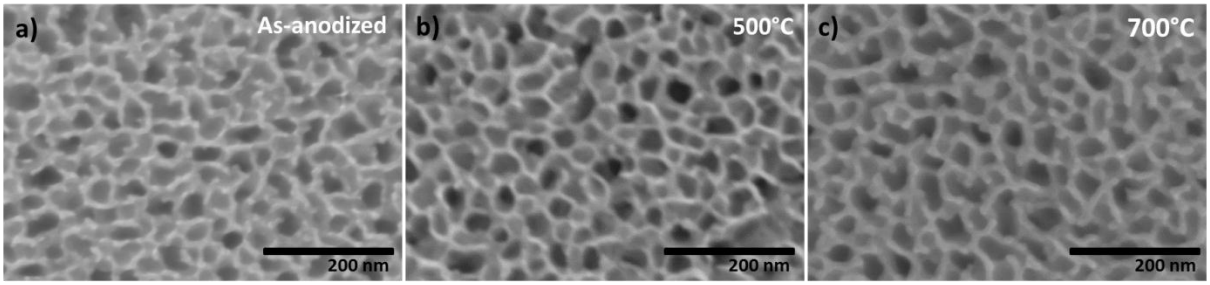

Fig. S2 SEM top-view images of samples prepared by anodizing an evaporated Sn layer (thickness ~ 600 nm) on p-type silicon wafer at 10 V in 0.2 M Na_2S and 0.1 M NH_4F electrolyte solution in 50 vol.% acetonitrile – 50 vol.% water mixture: a) as-formed, b) annealed at 500 °C and c) annealed at 700 °C.

Figure S3

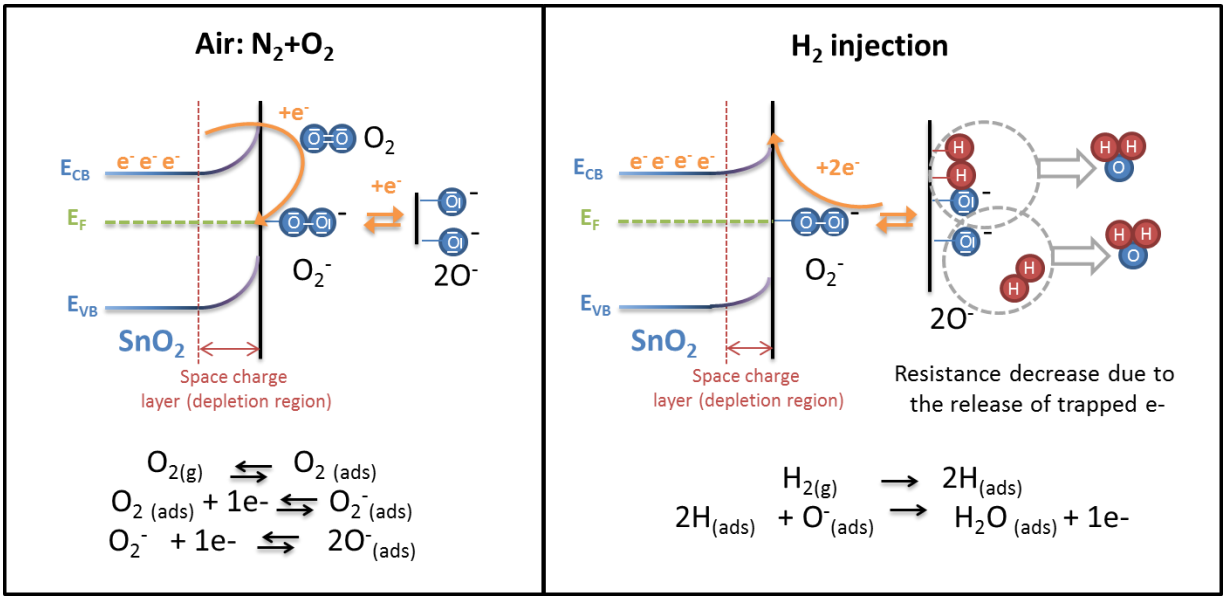

Fig. S3 Scheme of the sensing mechanism of SnO_2. In air conditions, oxygen is adsorbed at the surface of the oxide trapping electrons from the bulk. When the target gas (H_2) is injected in the chamber, adsorbed oxygen reacts with it forming water molecules and then the trapped electrons are released to the conduction band of the oxide causing the observed increase in the conductivity.

Figure S4

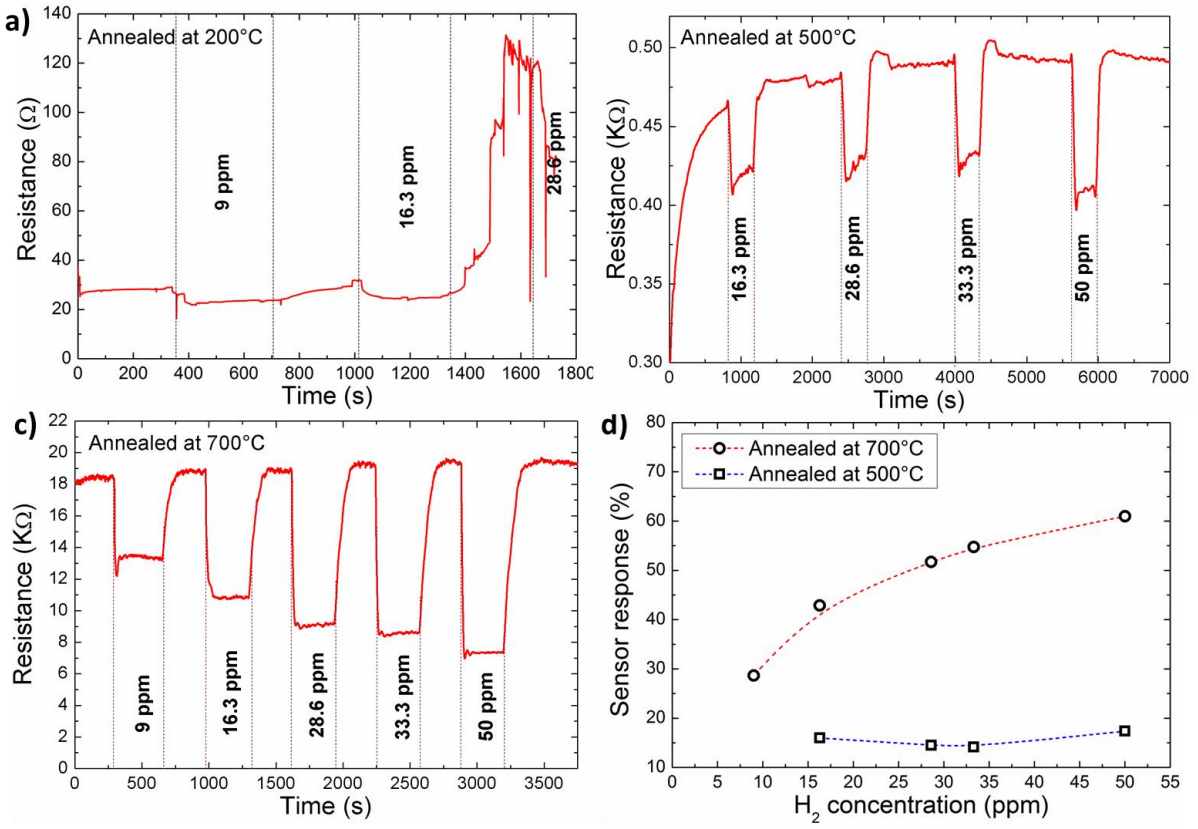

Fig. S4 a) Change in the resistance for the nanochannels anodic oxide film when exposed to H_2 concentrations ranging from 9 to 50 ppm (operating temperature = 120 °C). These films were prepared by anodizing a tin foil at an applied potential of 10 V for 10 minutes in a 50 vol.% acetonitrile - 50 vol.% H_2O solution containing 0.2 M Na_2S and 0.1 M NH_4F. Annealing of the layers was performed in air, at 200 °C for 1 h. b) Change in the resistance at 120 °C for a film prepared by anodizing a ~ 600 nm thick tin layer evaporated onto a Si wafer in the same electrolyte as for a) and annealed at 500 °C. c) Change in the resistance at 120 °C for an oxide film prepared by anodizing ~ 600 nm thick tin layer evaporated onto a Si in the same experimental conditions and then annealed at 700 °C. d) Sensor response of samples presented in b) and c) plotted as a function of the H_2 concentration.

Samples annealed at 200 °C presented very low resistance values (~ 25 Ω) in the presence of the reference stream (N_2+O_2 mixture) and no response was found when H_2 was introduced in the sensing chamber. Samples annealed at 500 °C exhibited higher resistance values (~ 470 Ω) and a slight decrease in resistance for H_2 concentrations in the range between 16 and 50 ppm. Here, the response was relatively low (*ca.* 15 %) and did not linearly increase with the increase of H_2 concentration. Best response was measured for samples annealed at 700 °C.

The conditions used for the sensing measurement are slightly different to the ones reported in Fig. 3 in the main text, so values of sensor response are not comparable.

Table S1

Magnitude of the sensor response (R_0/R_H) at the indicated operating temperatures for the different H_2 concentrations (in ppm)

SnO_2 thickness	**9 ppm H_2**	**16.3 ppm H_2**	**28.6 ppm H_2**	**33.3 ppm H_2**	**50 ppm H_2**
600 nm, 80 ºC	1.80	2.05	2.28	2.37	2.66
600 nm, 160 ºC	3.15	3.75	4.43	4.61	4.91
1.2 µm, 80 ºC	1.20	1.25	1.30	1.31	1.38
1.2 µm, 160 ºC	1.65	1.95	2.15	2.32	2.5

Figure S5

Evaporated Tin metal layers:

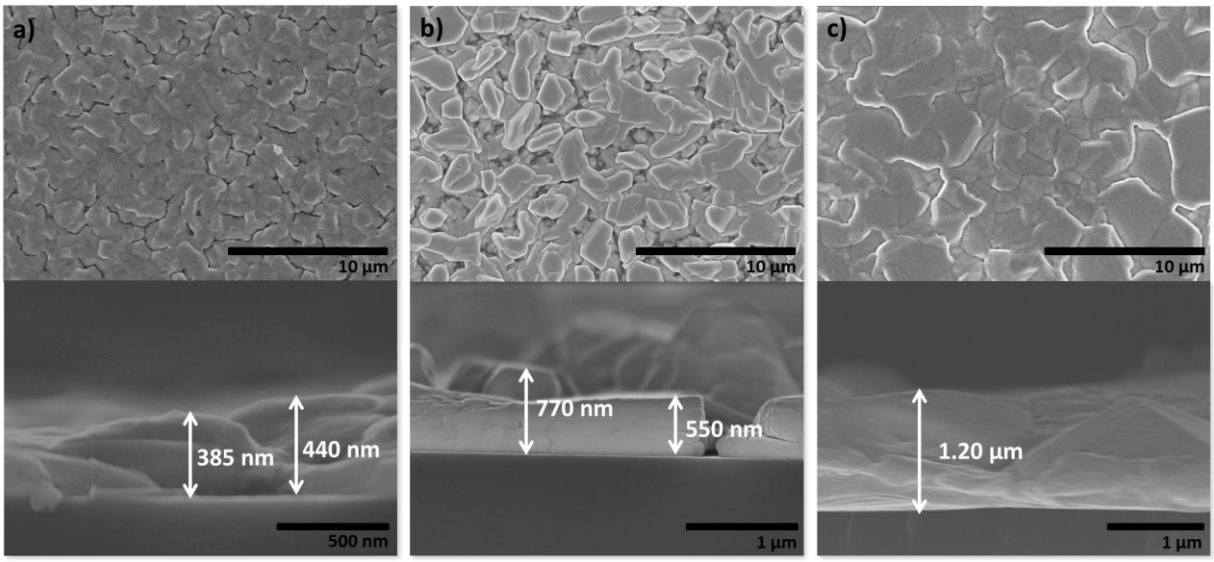

Fig. S5 SEM images of the top (top) and the cross-sectional view (bottom) of e-beam evaporated Sn layers on p-type Silicon substrates with different thicknesses: a) ~ 400 nm, b) ~ 600 nm and c) ~ 1.20 µm.

Figure S6

Sensing Setup and contact arrangement:

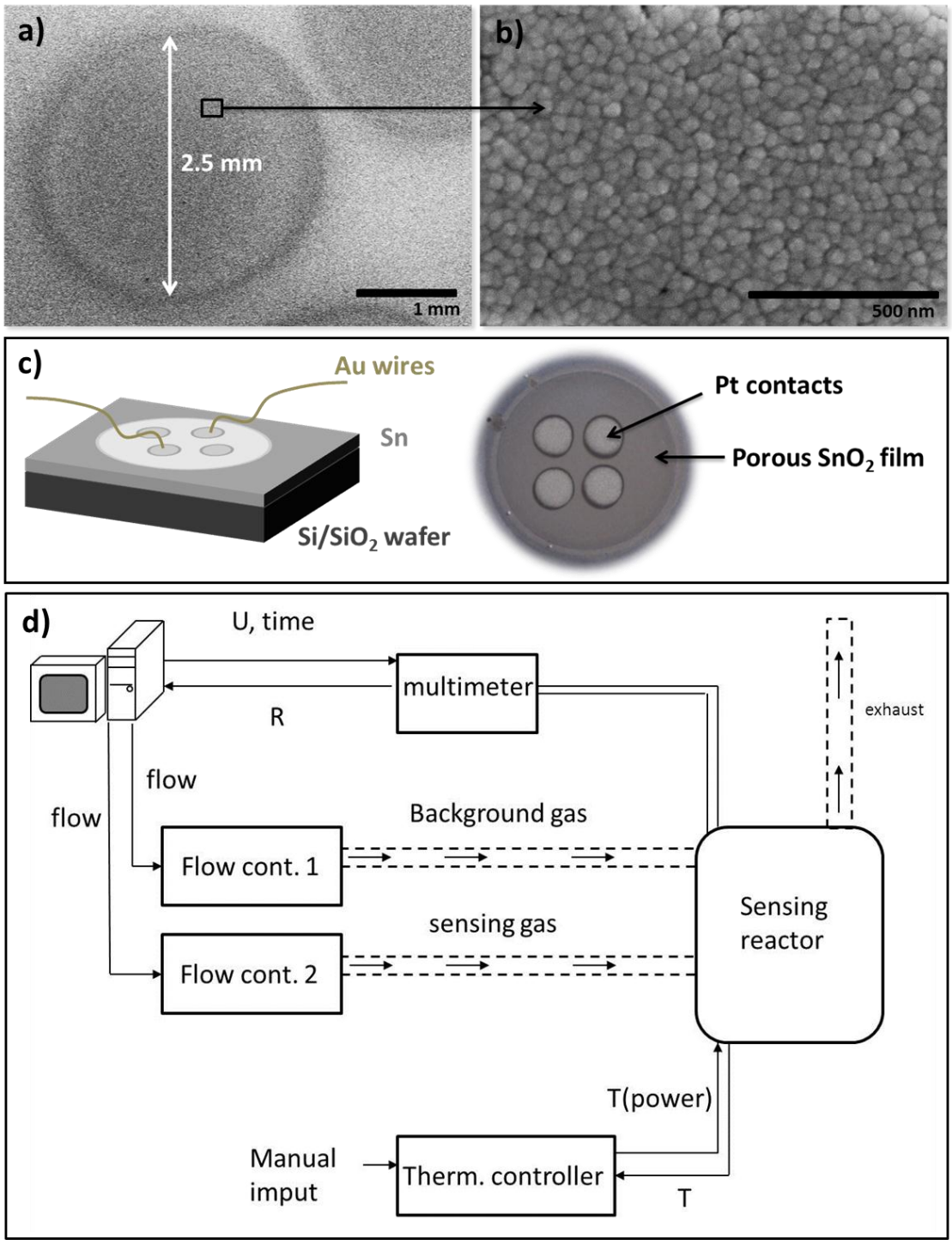

Fig. S6 a) SEM micrograph of the Pt contacts sputtered on top of an anodic oxide film for gas sensing measurements and b) high magnification SEM image of the Pt-coated surface. Scheme of c) the sensor and d) the sensing setup.

Figure S7

We found that an increase of the NH_4F concentration up to 0.1 M (by keeping constant the Na_2S concentration around 0.2 M) allows the formation of more open and defined pores at the top of the layer. On the other hand, with lower Na_2S concentrations (when the concentration of NH_4F was fixed at ~ 0.1 M) a black precipitate was formed and settled down at the top of the tin substrate. In these conditions, formation of a compact oxide layer along with localized pitting phenomena was the overall result.

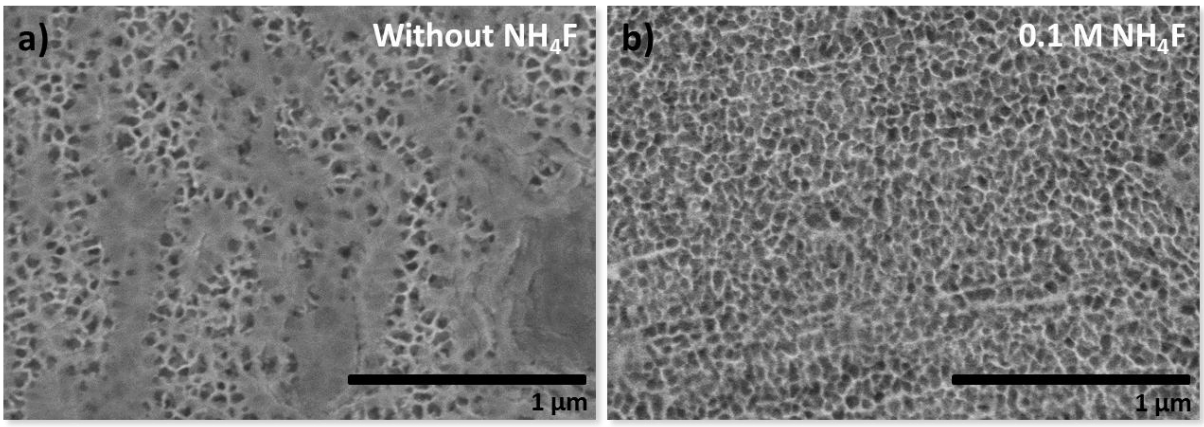

Fig. S7 Top view SEM micrograph of as-formed samples anodized at 5 V in a 20 vol.% Ethylene glycol - 80 vol.% water mixture containing 0.2 M Na_2S and a) no NH_4F and b) 0.1 M NH_4F. Anodization time was 30 min.

Figure S8

Several ripples along the inner cross-section of the anodic nanochannels can be observed in Fig. 1(b) and (c). The formation of these ripples is most probably induced by the high water content of the electrolyte which generates a fast growth rate of the anodic oxide (~ 0.8 - 0.9 μm min^{-1}).[1] Hence, anodization in electrolytes with a higher content of organic solvent were attempted in order to reduce the growth rate and to achieve higher degree of self-ordering together with smoother walls of the channels. However, a content of organic solvent around 50 vol.% was shown to be the most optimized condition. In fact, with contents between 60 and 80 %, pores resulted clogged at the top and channels were found to be less defined. Furthermore, only a thin compact oxide film was attained with electrolytes containing 80 to 100 vol.% of organic fraction.

However, anodization performed under the optimized conditions led to a significant drop of the current density during steady-state conditions. In fact, although much lower values in the range of ~ 1 mA cm^{-2} are reported for anodic TiO_2 nanotubes, steady-state current density values reported for anodization of tin in oxalic acid- or NaOH-based electrolytes were shown to be around 200 mA cm^{-2}.[2,3] Thus, in comparison to previous recipes for synthesizing anodic tin oxide, the relatively slow growth rate achieved with our electrolyte might be the reason for a more defined structure free of stacked layers and inner cracks.

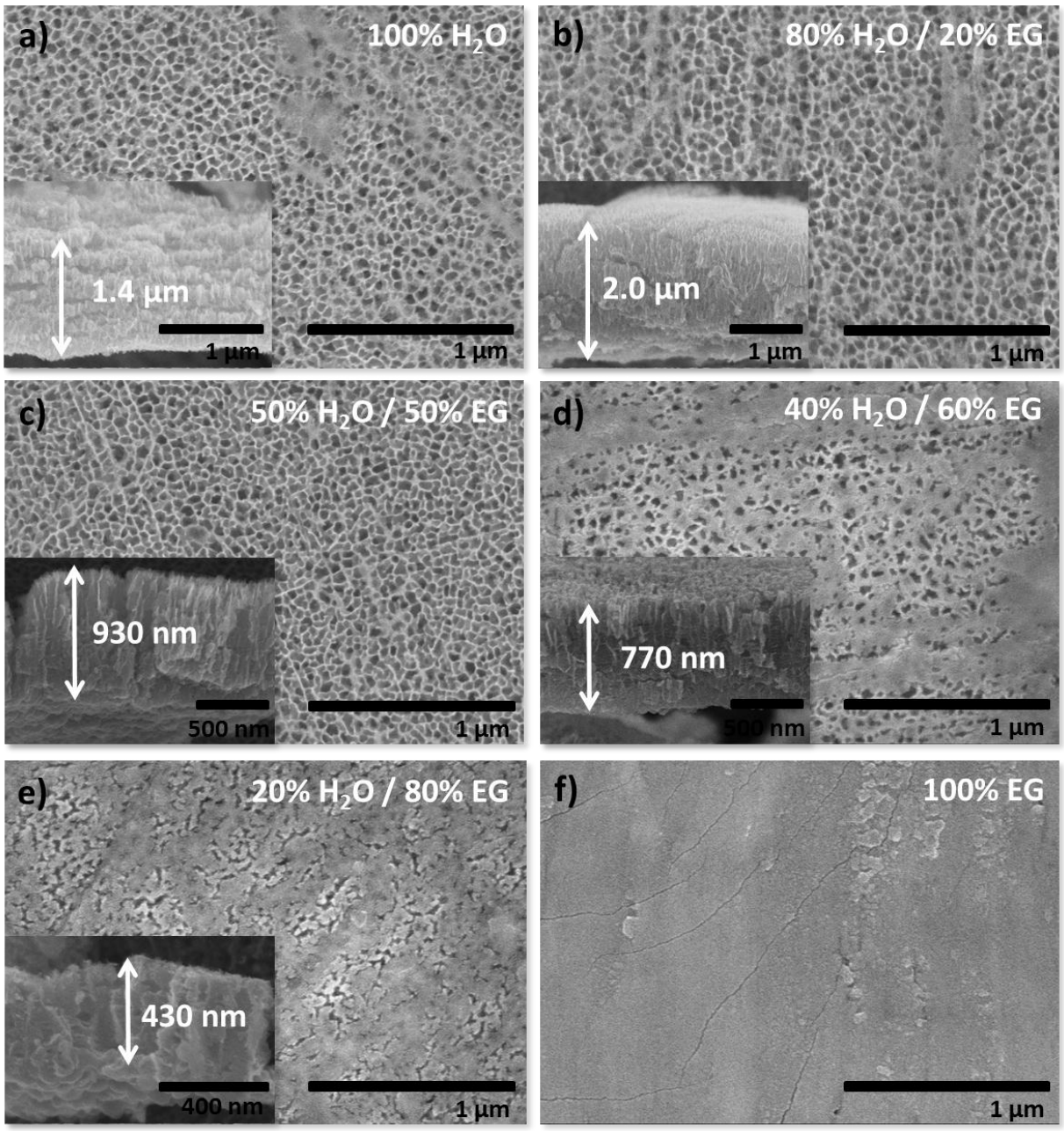

Fig. S8 SEM micrographs for the top and cross-sectional (inset) views for samples prepared by anodizing a tin foil at 5 V in 0.2 M Na_2S and 0.1 M NH_4F dissolved in a) 100 vol.% H_2O, b) 80 vol.% H_2O - 20 vol.% ethylene glycol, c) 50 vol.% H_2O - 50 vol.% ethylene glycol, d) 40 vol.% H_2O - 60 vol.% ethylene glycol, e) 20 vol.% H_2O - 80 vol.% ethylene glycol and f) 100 vol.% ethylene glycol. Anodization was performed for 10 minutes.

Figure S9

We found the anodization potential to have an important effect on the speed of the oxide formation. At 5V, the oxide growth rate was considerably reduced (~ 0.1 μm min^{-1}) but the nanochannel structures were no longer well defined as obtained when applying 10 V. On the contrary, a potential of 20 V led to the delamination of the films.

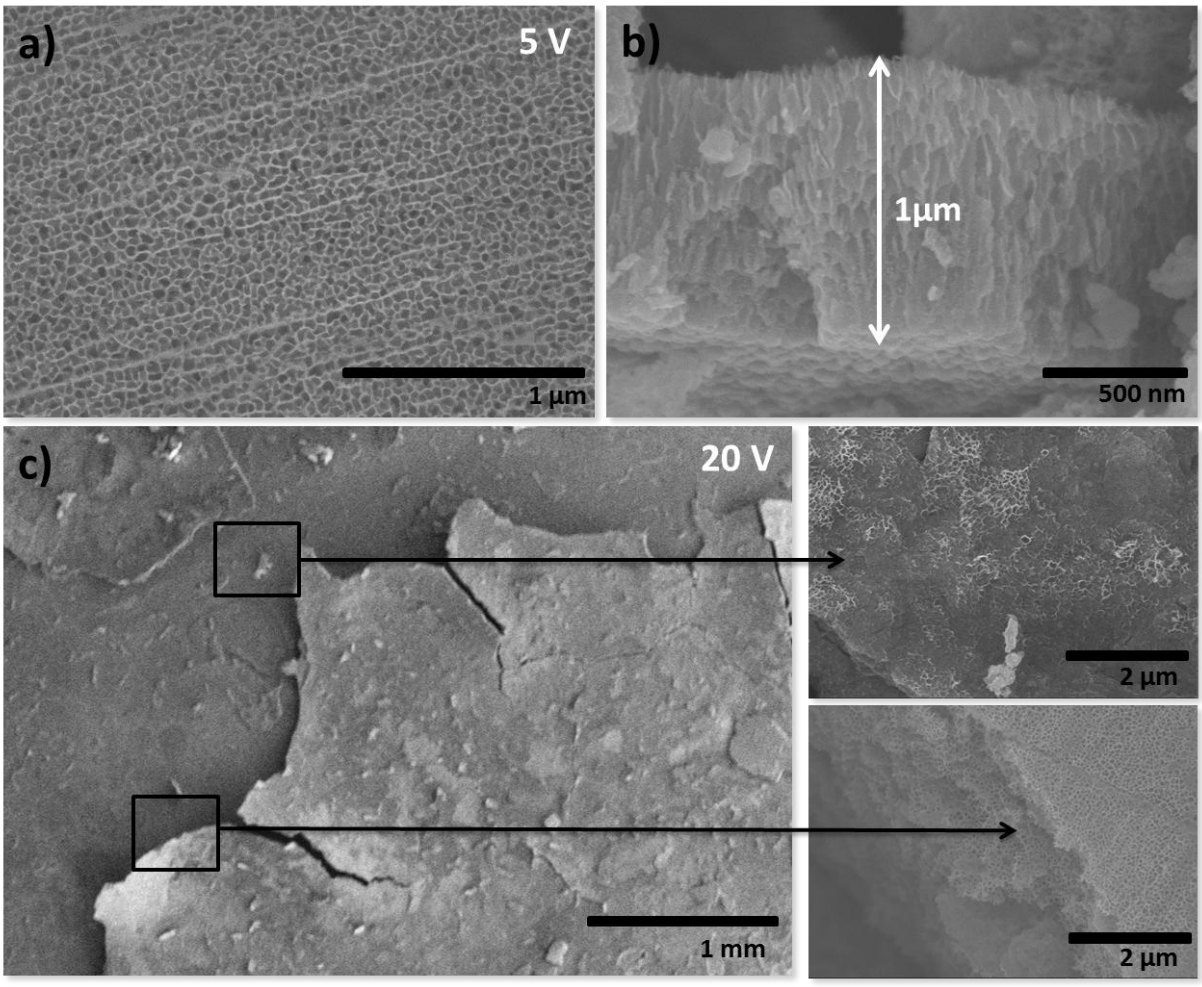

Fig. S9 SEM micrograph of a) top and b) cross-sectional views of a sample prepared by anodizing a Sn foil at 5 V for 10 minutes in 0.2 M Na_2S and 0.1 M NH_4F dissolved in a 50 vol.% acetonitrile – 50 vol.% water solvent. c) Top view SEM micrograph of a sample prepared in the same electrolyte by applying a potential of 20 V.

Figure S10

The cross-section of the anodic films resulted crack-free when such layers were grown up to a thickness of *ca.* 4.5 μm. Cracks along the structure of the anodic oxides started to form when the anodization was long-time lasting, this most likely owing to a more difficult removal of the O_2 bubbles from the nanochannels when the anodic layer becomes much thicker than just few microns. We also found that precipitate products formed at the top of the film when growing the anodic oxides up to 20 μm (this occurred after 30 min of anodization). For anodization times longer than 1h, the films peeled off from the substrate.

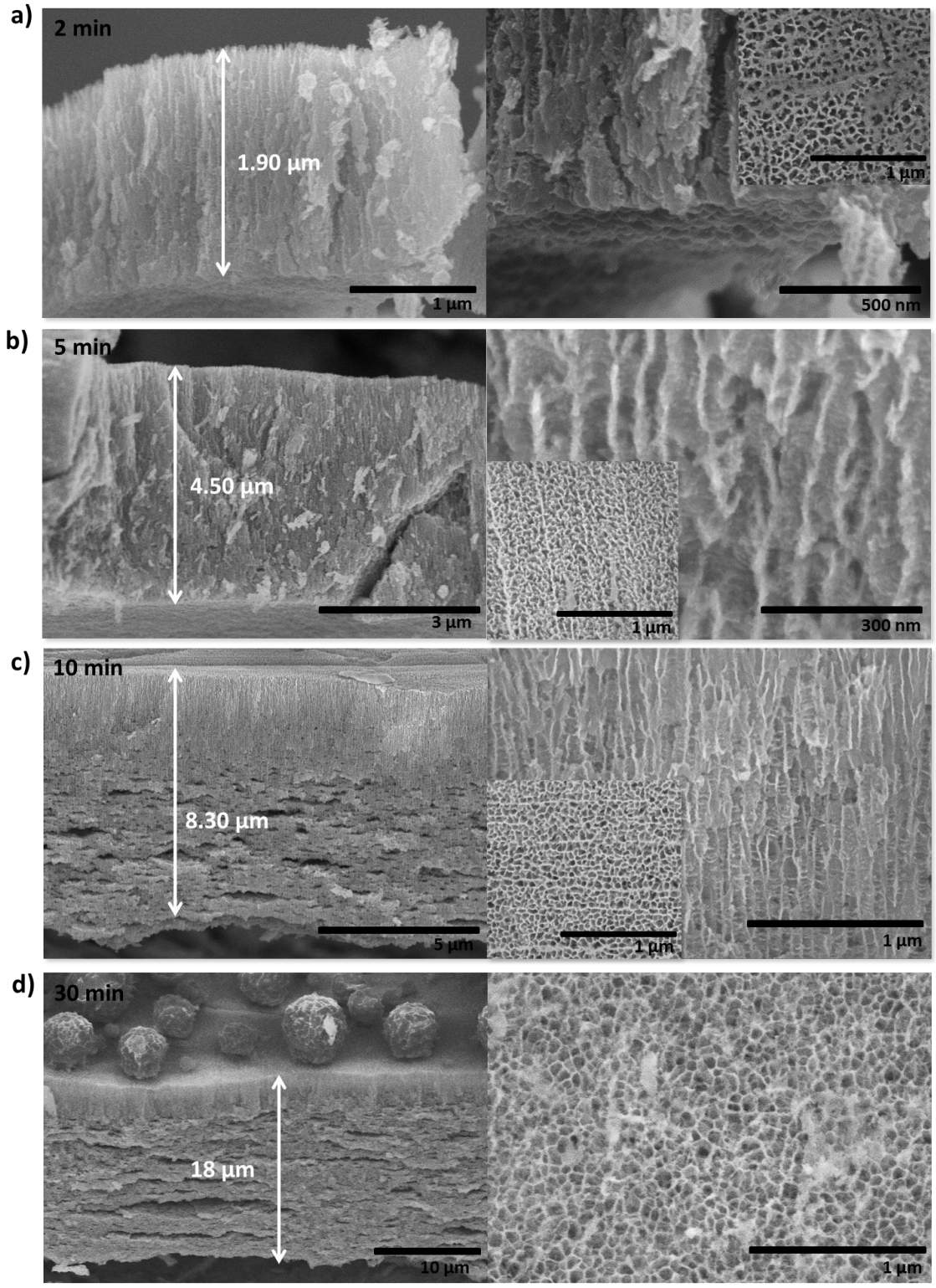

Fig. S10 SEM images of the cross-sectional view (left), details of the channels (right) and the top view (inset) of as-formed samples anodized at 10 V in an electrolyte composed of 50 vol.% acetonitrile and 50 vol.% water, containing 0.2 M Na_2S and 0.1 M NH_4F. Anodization experiments were carried out for a) 2 min, b) 5 min, c) 10 min and d) 30 min.

Figure S11

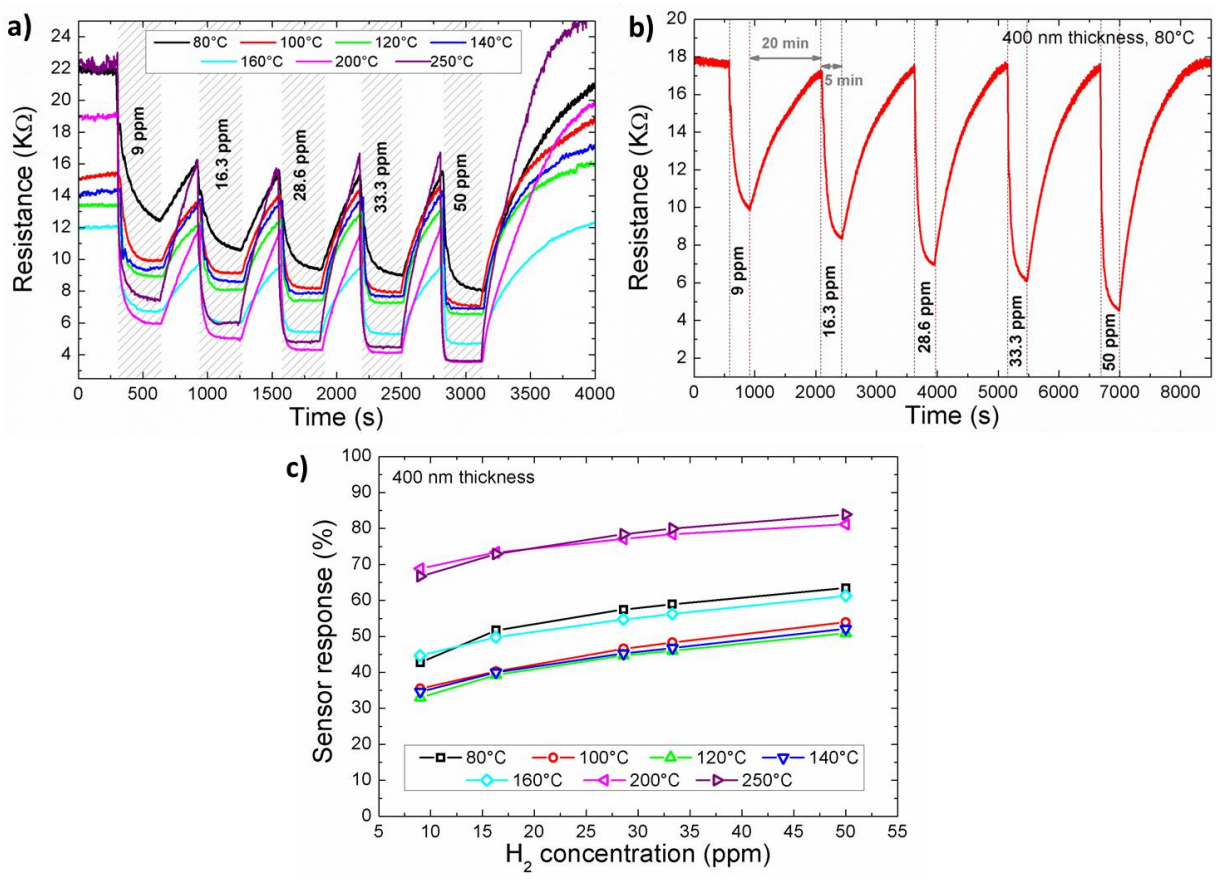

Fig. S11 a) Change in the resistance for a SnO_2 film exposed to different H_2 concentrations in the range of 9 to 50 ppm and by operating at several temperatures: 80, 100, 120, 140, 160, 200 and 250 °C. SnO_2 film was prepared by anodizing a ~ 400 nm thick tin layer evaporated onto Si wafer in a 50 vol.% acetonitrile - 50 vol.% H_2O solution containing 0.2 M Na_2S and 0.1 M NH_4F. The film was annealed at 700 °C. b) Change in resistance for a SnO_2 film prepared as in a) when exposed to different H_2 concentrations in the range of 9 to 50 ppm and by operating at 80ºC. As sensing response is slower at such operating temperature, the recovery time has been increased to 20 min. c) Sensor response dependence with the H_2 concentration for the same sample shown in a) when using different working temperatures.

Figure S12

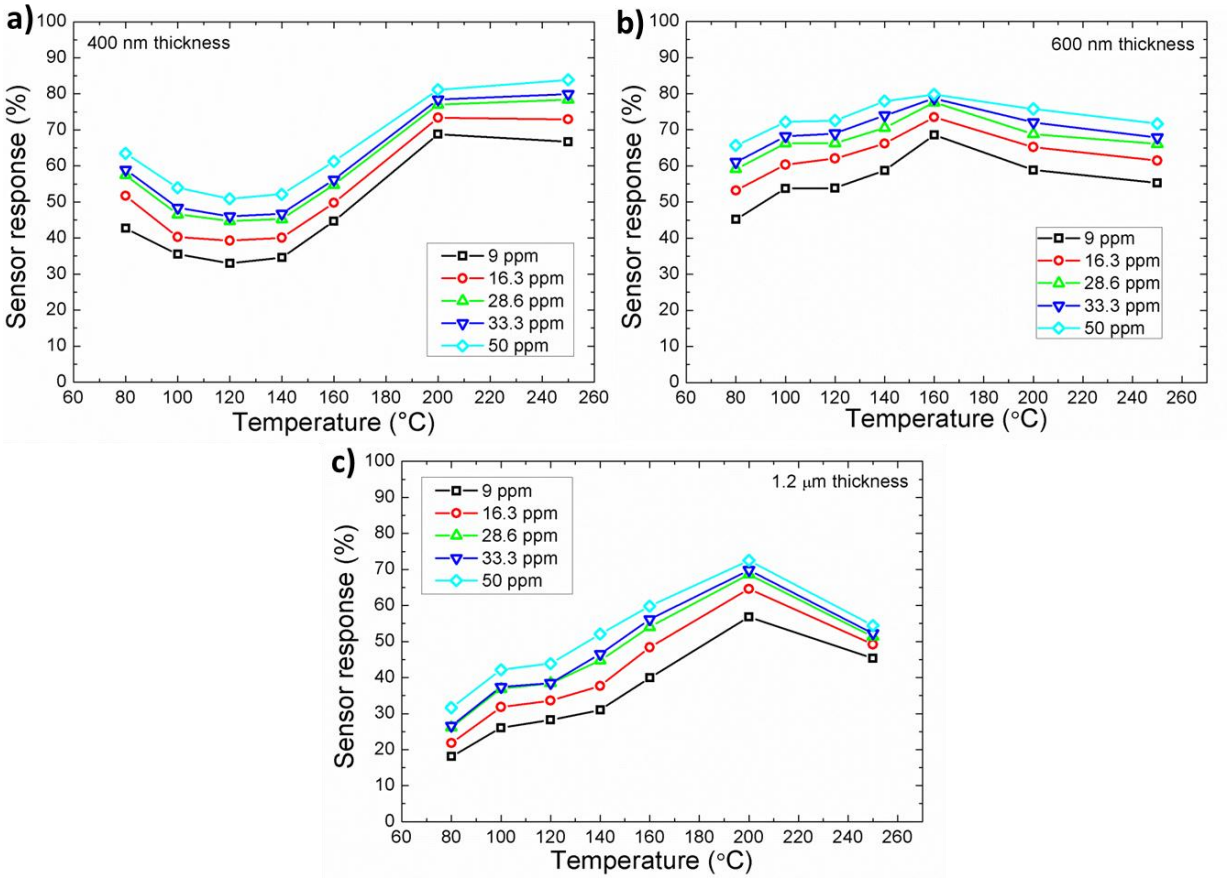

Fig. S12 Sensor response dependence with the operating temperature at H_2 concentrations of 9, 16.3, 28.6, 33.3, and 50 ppm for anodic SnO_2 films with a thickness of a) ~ 400 nm, b) ~ 600 nm and c) ~ 1.2 μm. All samples were prepared by anodizing an evaporated tin film in a 50 vol.% acetonitrile – 50 vol.% H_2O solution containing 0.2 M Na_2S and 0.1 M NH_4F and were annealed at 700°C.

Figure S13

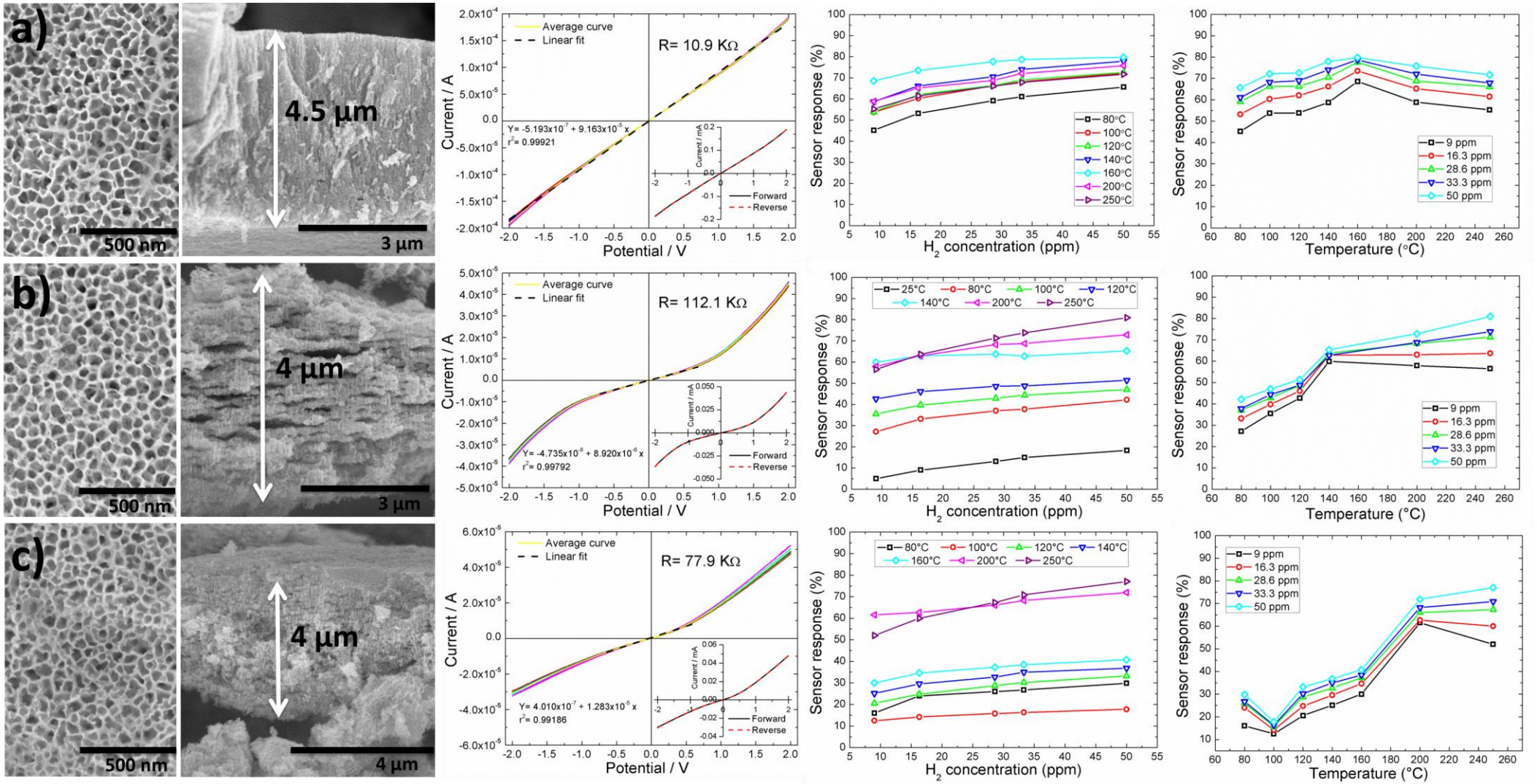

Fig. S13 From left to right: FESEM image of anodic layers prepared on Sn foil (top surface and cross-section view), I-V curves, sensor response at different H_2 concentrations and sensor response at different temperatures. Samples were prepared in different forms: a) in optimized conditions, using 50 vol.% acetonitrile - 50 vol.% H_2O solution containing 0.2 M Na_2S and 0.1 M NH_4F at 10 V, b) in non-optimized conditions by employing a 100% H_2O solution containing 0.2 M Na_2S and 0.1 M NH_4F at 10 V and c) 0.3 M oxalic acid at 8V as detailed in the literature [2]. In conditions b) and c) stacked layers are formed. I-V curves and sensing measurements were performed on anodic SnO_2 films of ~ 600 nm thick prepared by anodizing evaporated tin layers. All samples were annealed at 700ºC.

I-V curves between two gold contacts evaporated on the sample surface were taken at room temperature and in ambient conditions. The resistance of the films was calculated from the I-V curves. In these conditions, resistance (R) values might differ from the ones obtained when samples were mounted in the sensing setup due to the humidity in the air.

We found that resistance was higher for the samples prepared in non-optimized conditions (Fig.S13b and c). This can be attributed to the inner cracks they present. Although all films show a remarkable response to H_2, at low operating temperatures the response is much better in samples prepared under optimized conditions (Fig.S13a) maybe due to their better conducting properties. Moreover, these films seem to present a more stable response though all the temperature range under study.

Figure S14

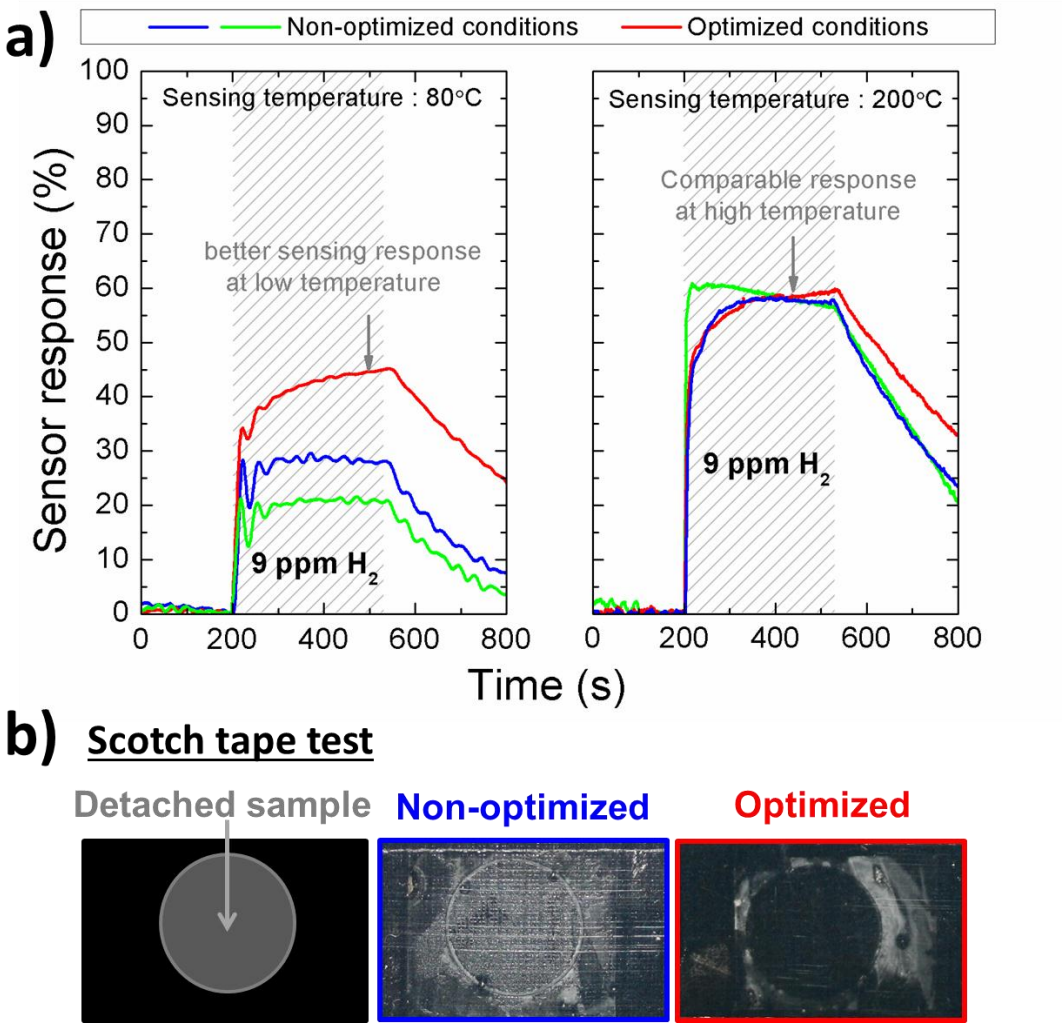

Fig. S14 a) Comparison between the sensor response at 80ºC and 200ºC for samples prepared in optimized (50 vol.% acetonitrile - 50 vol.% H_2O solution containing 0.2 M Na_2S and 0.1 M NH_4F at 10 V) and non-optimized (100% H_2O solution containing 0.2 M Na_2S and 0.1 M NH_4F at 10 V (blue); 0.3 M oxalic acid at 8V (green)) conditions. b) Photograph of the detached film after performing the Scotch tape test in samples prepared in optimized and non-optimized conditions. Samples prepared in optimized conditions show a better mechanical stability.

References:

1. P. Roy, S. Berger, P. Schmuki, Angew. Chem. Int. Ed. 50 (2011) 2904.
2. L. Zaraska, N. Czopic, M. Bobruk, G. D. Sulka, J. Mech, M. Jaskula, Electrochim. Acta 104 (2013) 549.
3. J.-W. Lee, S.-J. Park, W.-S. Choi, H.-C Shin, Electrochim. Acta 56 (2011) 5919.